Principles of Terahertz Science and Technology

Yun-Shik Lee

Principles of Terahertz Science and Technology

Springer

Yun-Shik Lee
Physics Department
Oregon State University
Corvallis, Oregon 97331
USA

ISBN 978-0-387-09539-4 e-ISBN 978-0-387-09540-0

Library of Congress Control Number: 2008935382

Printed on acid-free paper.

9 8 7 6 5 4 3 2 1

springer.com

To my parents Su-Ho Lee and Soon-Im Shin

Preface

Over the last two decades, THz technology has ripened enough that a thorough summary and review of the relevant topics is in order. Many different disciplines such as ultrafast spectroscopy, semiconductor device fabrication, and bio-medical imaging involve the recent development of THz technology. It is an important task to lay down a common ground among the researchers, so that they can communicate smoothly with one another. Besides, the THz community is growing fast and the THz technology is in a transitional period. The THz research activities have mainly focused on generation and detection until lately, but the focal point has shifted to the practical applications such as high-speed communication, molecular spectroscopy, security imaging, and medical diagnosis, among many others.

This book covers a broad range of topics and fundamental issues. Individuals from distinct disciplines have helped developing new THz technologies, and in order to reach the next level, i.e., practical applications, the technology requires its researchers to understand and communicate with one another. This book serves this general purpose by providing the researchers with a common reference, thus bridging "the THz gap".

I have tried to elucidate the fundamentals of THz technology and science for their potential users. This book surveys major techniques of generating, detecting, and manipulating THz waves. It also discusses a number of essential processes where THz waves interact with physical, chemical, and biological systems. Scientists and engineers of various disciplines realize that the THz gap in the electromagnetic spectrum is now accessible thanks to the recent advances in THz source and detection technologies. Many are seeking ways by which they can incorporate the new technologies into their expertise and research agenda. Younger researchers, who wish or are to join THz research groups, would also find this new field challenging due to many barriers, the lack of comprehensive introduction and/or instruction among them. Potential users of THz technology should be prepared in the essential concepts and techniques of THz science and technology; I hope this book be an introductory guide for the new comers.

During the process of writing this book, many colleagues, friends, and students gave me worthy criticism and introduction. Although it is impossible to acknowledge all scientific contributions, I am deeply grateful of those whose works I use in this book. I am much obliged to Joe Tomaino, Andy Jameson, and Jeremy Danielson for their invaluable advice. I am indebted to the National Science Foundation and the Alexander von Humboldt-Foundation for their generous support. Finally, I thank my wife, JungHwa, for her support in every possible ways.

Corvallis
September 2008 *Yun-Shik Lee*

Contents

1

Introduction

Terahertz (THz) radiation is electromagnetic radiation whose frequency lies between the microwave and infrared regions of the spectrum. We cannot see THz radiation, but we can feel its warmth as it shares its spectrum with far-infrared radiation. Naturally occurring THz radiation fills up the space of our everyday life, yet this part of the electromagnetic spectrum remains the least explored region mainly due to the technical difficulties involved in making efficient and compact THz sources and detectors. The lack of suitable technologies led to the THz band being called the "THz gap". This technological gap has been rapidly diminishing for the last two decades. Optical technologies have made tremendous advances from the high frequency side, while microwave technologies encroach up from the low frequency side. This chapter gives a brief perspective on the basic properties of THz radiation and its interaction with materials, which lays down the foundation to discuss the progress of THz science and technology in subsequent chapters.

1.1 Terahertz Band

"Terahertz radiation" is the most common term used to refer to this frequency band, analogous to microwaves, infrared radiation, and x-rays. It is rather awkward to use a frequency unit for naming a spectral band. Nevertheless, as "terahertz" has become a symbolic word designating the entire field, we will universally use this term throughout this book. An alternative and seemingly better terminology is "T-rays", where "T" stands for terahertz. It was initially coined for an imaging technique, and will be used in Chapter 7, which is dedicated to T-ray imaging technologies and applications.

Until quite recently, THz technologies had been independently developed by researchers from several different disciplines. In practice, different communities use different units to describe the spectrum of THz radiation. We will use THz (10^{12} Hz) as the universal unit in this book, but other units

will also be used when they are appropriate. Frequently used units and their conversions at 1 THz are as follows:

- Frequency: $\nu = 1$ THz $= 1000$ GHz
- Angular frequency: $\omega = 2\pi\nu = 6.28$ THz
- Period: $\tau = 1/\nu = 1$ ps
- Wavelength: $\lambda = c/\nu = 0.3$ mm $= 300$ μm
- Wavenumber: $\bar{k} = k/2\pi = 1/\lambda = 33.3$ cm^{-1}
- Photon energy: $h\nu = \hbar\omega = 4.14$ meV
- Temperature: $T = h\nu/k_B = 48$ K

where c is the speed of light in vacuum, h is Plank's constant, and k_B is Boltzmann's constant. Physicists tend to use μm and meV as units of photon wavelength and energy, respectively; chemists use cm^{-1} as a unit of wavenumber; engineers use mm and GHz as units of wavelength and frequency, respectively. In physics, angular wavenumber ($k = 2\pi/\lambda$) is usually abbreviated as wavenumber. In this book, we will use the abbreviated notation when it is clearly defined.

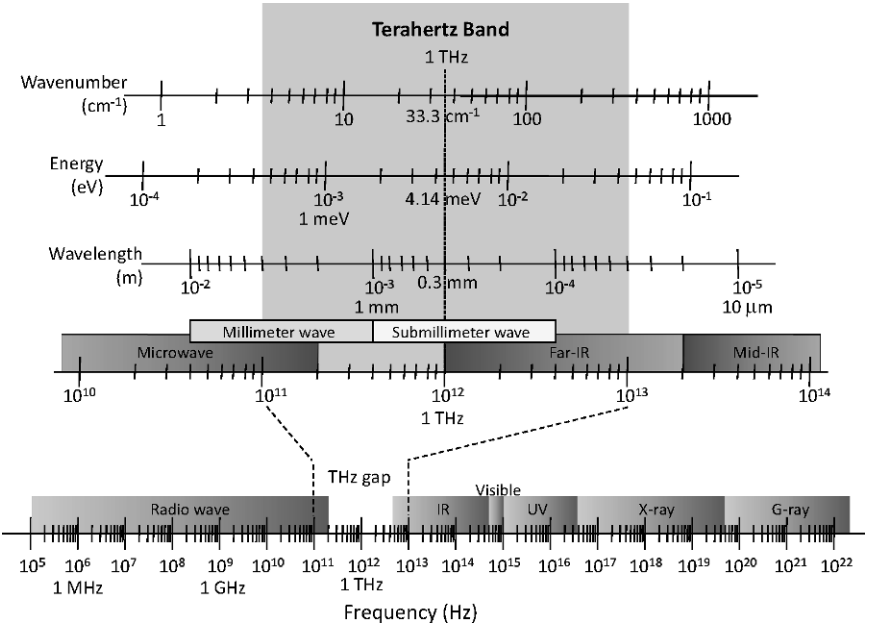

Fig. 1.1. Terahertz band in the electromagnetic spectrum

The THz band does not have a standard definition yet. Commonly used definitions are included in the spectral region between 0.1 and 30 THz. The range of 10-30 THz, however, exceeds the far-IR band and intrudes on the mid-IR band, where well established optical technologies exist. Unless we deal with

ultrabroadband THz pulses, we will use 0.1-10 THz as a universal definition of the THz band. Figure 1.1 illustrates the THz band in the electromagnetic spectrum. The THz band merges into neighboring spectral bands such as the millimeter-wave band, which is the highest radio frequency band known as Extremely High Frequency (EHF), the submillimeter-wave band, and the far-IR band. The definitions of these bands are as follows:

- Millimeter wave (MMW): 1-10 mm, 30-300 GHz, 0.03-0.3 THz
- Submillimeter wave (SMMW): 0.1-1 mm, 0.3-0.3 THz
- Far infrared radiation (Far-IR): (25-40) to (200-350) μm, (0.86-1.5) to (7.5 to 12) THz
- Sub-THz radiation: 0.1-1 THz

These bands are also distinguished by their characteristic technologies. Millimeter wave emitters and sensors are solid-state devices based on microwave technologies. Traditionally, far-IR applications rely on optical and thermal devices.

1.2 Terahertz Generation and Detection

Technological advances in optics and electronics have resulted in many different types of THz sources and sensors. Chapters 3 and 4 are devoted to broadband and continuous-wave (CW) THz technologies, which are classified by similarities in radiation characteristics. In this section, we make brief descriptions of the schemes used for THz generation and detection, grouped by operational concepts.

1.2.1 Terahertz Sources

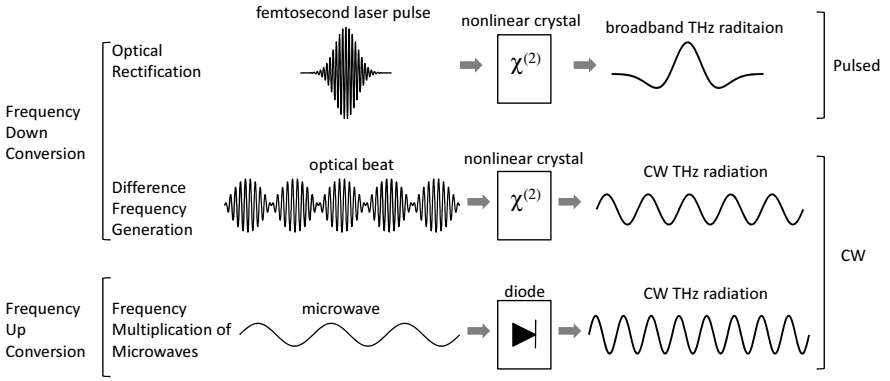

Fig. 1.2. Terahertz generation in nonlinear media

One way of generating THz radiation is to exploit a nonlinear medium in which incident electromagnetic waves undergo nonlinear frequency conversion (Fig. 1.2). Optical rectification and difference frequency generation (DFG) are second order nonlinear optical processes in which a THz photon at frequency ω_T is created by interaction of two optical photons at frequencies ω_1 and ω_2 with a nonlinear crystal, such that $\omega_T = \omega_1 - \omega_2$. Femtosecond laser pulses with a broad spectrum (bandwidth∼10 THz) generate broadband THz pulses, whose shape resembles the optical pulse envelope, via optical rectification. Two CW optical beams produce CW THz radiation by DFG. Solid-state THz sources based on microwave technology convert incoming microwaves into their harmonic waves utilizing diodes with strongly nonlinear I-V characteristics.

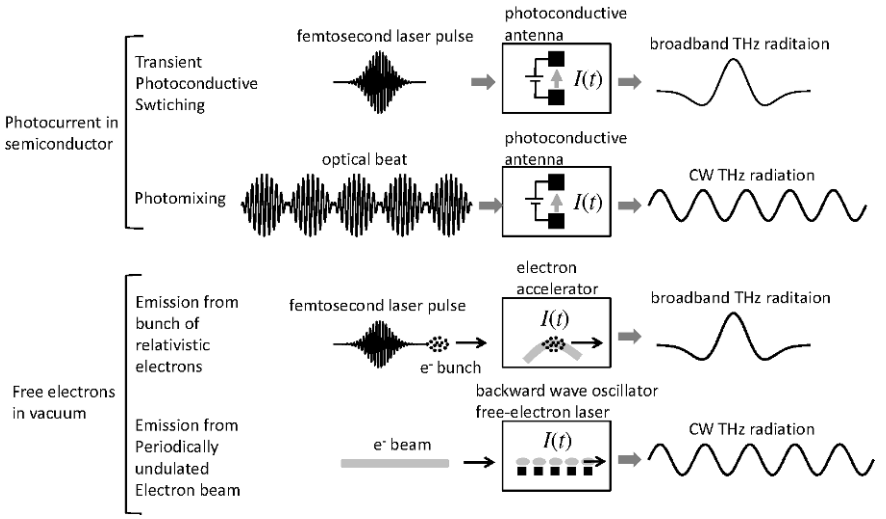

Fig. 1.3. THz radiation from accelerating electrons

Accelerating charges, and time-varying currents, radiate electromagnetic waves (Fig. 1.3). THz radiation can be generated from a biased photoconductive (PC) antenna excited by laser beams. A PC antenna consists of two metal electrodes deposited on a semiconductor substrate. An optical beam, illuminating the gap between the electrodes, generates photocarriers, and a static bias field accelerates the free carriers. This photocurrent varies in time corresponding to the incident laser beam intensity. Consequently, femtosecond laser pulses produce broadband THz pulses. Mixing two laser beams with different frequencies forms an optical beat, which generates CW THz radiation at the beat frequency. This technique is called photomixing.

Electron accelerators produce extremely bright THz radiation using relativistic electrons. A femtosecond laser pulse triggers an electron source to

generate a ultrashort pulse of electrons. After being accelerated to a relativistic speed, the electrons are smashed into a metal target, or are forced into circular motion by a magnetic field. Coherent THz radiation is generated by this transient electron acceleration.

Backward wave oscillators (BWOs) are laboratory-size equipment, and free-electron lasers (FELs), small scale electron accelerators, are large facilities. In spite of the huge difference in size, there is a similarity in their THz generation mechanism. In both, an electron beam is undulated by a periodic structure: a BWO has a metal grating and a FEL consists of a magnet array. CW THz radiation is produced by the periodic acceleration of electrons.

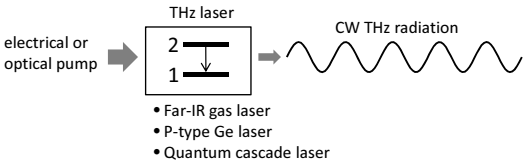

Fig. 1.4. THz emission from laser

Laser action requires a population-inverted two-level quantum system (Fig. 1.4). Far-IR gas lasers utilize molecular rotation energy levels, whose transition frequencies fall into the THz region. P-type germanium lasers are electrically pumped solid-state lasers. Their lasing action relies on the population inversion of two Landau levels formed by hot-carriers submerged in crossed electric and magnetic fields. Quantum cascade lasers (QCLs) are semiconductor heterostructure lasers consisting of periodically alternating layers of dissimilar semiconductors. Transitions between subbands of these semiconductor nanostructures involve THz photons. In a QCL, electrons undergo successive intersubband transitions to generate coherent THz radiation.

1.2.2 Terahertz Detectors

THz detection schemes are largely classified as either coherent or incoherent techniques. The fundamental difference is that coherent detection measures both the amplitude and phase of the field, whereas incoherent detection measures the intensity. Coherent detection techniques are closely associated with generation techniques in that they share underlying mechanisms and key components. In particular, optical techniques utilize the same light source for both generation and detection.

Figure 1.5 illustrates the commonly used coherent detection schemes. Free-space electro-optic (EO) sampling measures the actual electric field of broadband THz pulses in the time domain by utilizing the Pockels effect, which is closely related to optical rectification. A THz field induces birefringence in a nonlinear optical crystal which is proportional to the field amplitude. The

entire waveform is determined by a weak optical probe measuring the field-induced birefringence as a function of the relative time delay between the THz and optical pulses.

Sensing with a PC antenna also measures broadband THz pulses in the time domain. In the absence of a bias field, a THz field induces a current in the photoconductive gap when an optical probe pulse injects photocarriers. The induced photocurrent is proportional to the THz field amplitude. The THz pulse shape is mapped out in the time domain by measuring the photocurrent while varying the time delay between the THz pulse and the optical probe.

A combined setup of broadband THz generation and detection measures changes in both the amplitude and phase of THz pulses induced by a sample, which provides enough information to simultaneously determine the absorption and dispersion of the sample. This technique is named THz time-domain spectroscopy, or, in short, THz-TDS.

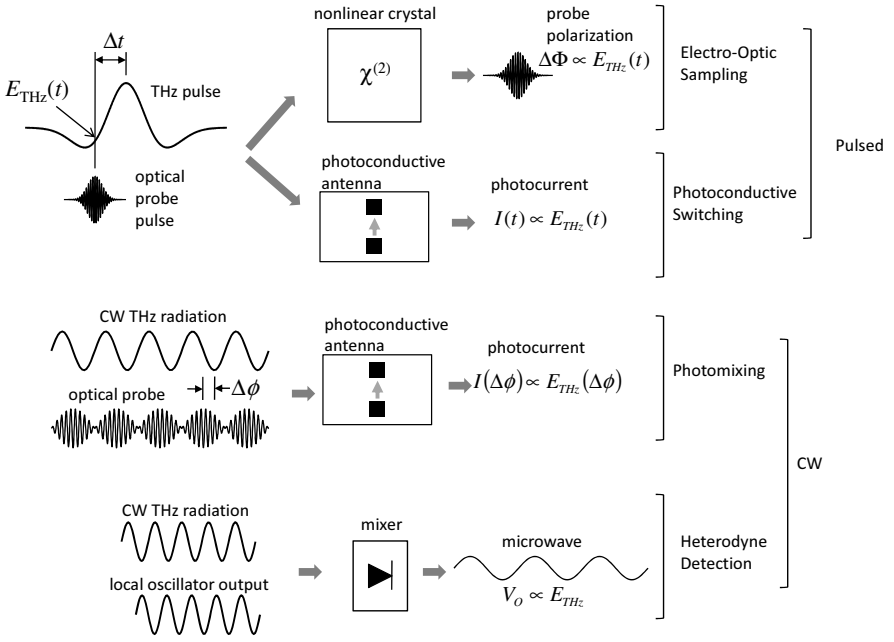

Fig. 1.5. Coherent detection of THz radiation

Photomixing measures CW THz radiation by exploiting photoconductive switching. In this case, the photocurrent shows sinusoidal dependence on the relative phase between the optical beat and the THz radiation.

Heterodyne detection utilizes a nonlinear device called a "mixer". Schottky diodes are commonly used as mixers. The key process in a mixer is frequency downconversion, which is carried out by mixing a THz signal ω_s with reference

radiation at a fixed frequency ω_{LO}. The mixer produces an output signal at the difference frequency called the "intermediate frequency", $\omega_D = |\omega_S - \omega_{LO}|$. The amplitude of the output signal is proportional to the THz amplitude. Unlike the optical techniques, heterodyne detection is usually used to detect incoherent radiation.

Commonly used incoherent detectors are thermal sensors such as bolometers, Golay cells, and pyroelectric devices. A common element of all thermal detectors is a radiation absorber attached to a heat sink. Radiation energy is recorded by a thermometer measuring the temperature increase in the absorber. Each type of thermal detector is distinguished by its specific scheme used to measure the temperature increase. Bolometers are equipped with an electrical resistance thermometer made of a heavily doped semiconductor such as Si or Ge. In general, bolometers operate at cryogenic temperature. Pyroelectric detectors employ a pyroelectric material in which temperature change gives rise to spontaneous electric polarization. In a Golay cell, heat is transferred to a small volume of gas in a sealed chamber behind the absorber. An optical reflectivity measurement detects the membrane deformation induced by the pressure increase. These thermal detectors respond to radiation over a very broad spectral range. Because a radiation absorber must reach to thermal equilibrium for a temperature measurement, detection response is relatively slow compared with typical light detectors.

1.3 Terahertz Applications

The THz region is crowded by innumerable spectral features associated with fundamental physical processes such as rotational transitions of molecules, large-amplitude vibrational motions of organic compounds, lattice vibrations in solids, intraband transitions in semiconductors, and energy gaps in superconductors. THz applications exploit these unique characteristics of material responses to THz radiation.

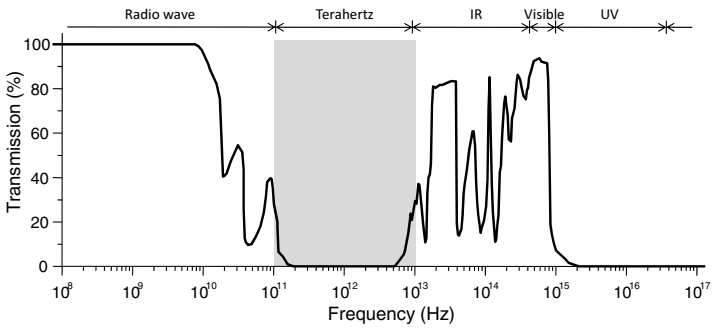

Fig. 1.6. Atmospheric transmission spectrum of electromagnetic waves

Compared with the neighboring regions of radio waves and infrared radiation, the THz band shows exceedingly high atmospheric opacity due to the rotational lines of constituent molecules (Fig. 1.6). In particular, absorption by water vapor is the predominant process of atmospheric THz attenuation. Figure 1.7 shows a high-resolution transmission spectrum of water vapor. In practice, water absorption is an important factor to be considered when designing an operation scheme for a THz application.

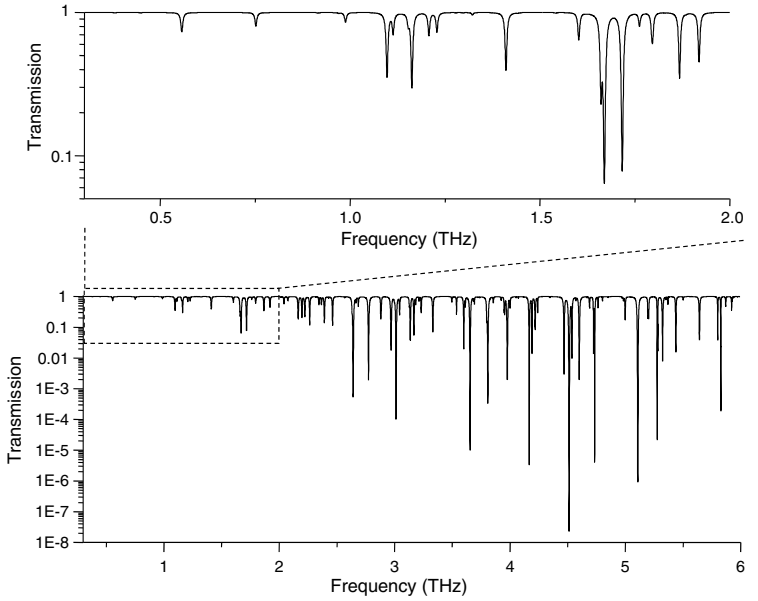

Fig. 1.7. Water vapor transmission spectrum from 0.3 to 6 THz

Distinctive line structures of each molecular species can be utilized to identify it in an unknown specimen. Furthermore, spectral line-shapes provide crucial information concerning microscopic mechanisms of molecular collisions. High-resolution THz spectroscopy is being used to monitor the Earths atmosphere and to observe molecules in the interstellar medium.

Spectral signatures of organic and biological molecules in the THz region are associated with large amplitude vibrational motions and inter-molecular interactions. THz spectroscopy is capable of analyzing these molecular dynamics, it can therefore be applied to the detection of explosives and illicit drugs, testing pharmaceutical products, investigating protein conformation, etc.

Based on optical properties at THz frequencies, condensed matter is largely grouped into three types: water, metal, and dielectric. Water, a strongly polar liquid, is highly absorptive in the THz region. Because of high electrical

conductivity, metals are highly reflective at THz frequencies. Nonpolar and nonmetallic materials, i.e., dielectrics such as paper, plastic, clothes, wood, and ceramics that are usually opaque at optical wavelengths, are transparent to THz radiation. A brief description of the optical properties of each material type is shown in Table 1.1.

Table 1.1. Optical Properties of Condensed Matter in the THz Band

Material Type	Optical Property
liquid water	high absorption ($\alpha \approx 250$ cm^{-1} at 1 THz)
metal	high reflectivity (>99.5% at 1 THz)
plastic	low absorption ($\alpha < 0.5$ cm^{-1} at 1 THz)
	low refractive index ($n \approx 1.5$)
semiconductor	low absorption ($\alpha < 1$ cm^{-1} at 1 THz)
	high refractive index ($n \sim$ 3-4)

These stark contrasts of THz properties are useful for many imaging applications. Since common packaging materials are dielectric, THz imaging is applied to nondestructive testing to inspect sealed packages. Because of the high absorption of water in the THz region, hydrated substances are easily differentiated from dried ones. Metal objects also can be easily identified due to their high reflectivity and complete opacity. The same concept is applied to security applications. THz imaging is used to identify weapons, explosives, and illegal drugs concealed underneath typical wrapping and packaging materials. The high sensitivity of THz radiation to water is useful for medical applications because, in a biological system, small changes in water content could indicate crucial defects emerging in the region.

In addition to the applications we briefly described in this section, THz spectroscopy and imaging techniques have been applied to many others ranging from basic scientific missions to commercial projects. We will look into them in following chapters.

2

Basic Theories of Terahertz Interaction with Matter

This chapter is concerned with basic concepts and theories that form the foundation for understanding the unique characteristics of THz radiation and its interaction with materials. Classical electromagnetic theory provides a general description of THz waves which propagate in and interact with macroscopically uniform media. The basic framework of quantum theory is utilized to describe elementary exciations at THz frequencies.

2.1 Electromagnetic Waves in Matter

We shall begin with Maxwell's equations to describe THz waves as we would do for any other spectral regions. The macroscopic form of Maxwell's equations have the form

$$\nabla \cdot \mathbf{D} = \rho_f, \tag{2.1}$$

$$\nabla \cdot \mathbf{B} = 0, \tag{2.2}$$

$$\nabla \times \mathbf{E} = -\frac{\partial \mathbf{B}}{\partial t}, \tag{2.3}$$

$$\nabla \times \mathbf{H} = \mathbf{J}_f + \frac{\partial \mathbf{D}}{\partial t}, \tag{2.4}$$

where ρ_f and $\mathbf{J}_f$ are the free charge density and the free current density. These deceptively simple equations, together with the Lorentz force law

$$\mathbf{F} = q\left(\mathbf{E} + \mathbf{v} \times \mathbf{B}\right), \tag{2.5}$$

constitute the entire theoretical basis of classical electrodynamics. The macroscopic fields $\mathbf{D}$ and $\mathbf{H}$ are related to the fundamental fields $\mathbf{E}$ and $\mathbf{B}$ as

$$\mathbf{D} \equiv \epsilon_0 \mathbf{E} + \mathbf{P} = \epsilon \mathbf{E}, \tag{2.6}$$

$$\mathbf{H} \equiv \frac{1}{\mu_0}\mathbf{B} - \mathbf{M} = \frac{1}{\mu}\mathbf{B}, \tag{2.7}$$

where ϵ_0 and μ_0 are the permittivity and the permeability of free space. The polarization $\mathbf{P}$ and the magnetization $\mathbf{M}$ contain the information about the macroscopic-scale electromagnetic properties of the matter. The last terms in Eqs. 2.6 and 2.7, where ϵ and μ denote the the electric permittivity and the magnetic permeability, are valid only if the media is isotropic and linear. Typical magnetic responses of matter are subtle, $|\mu - \mu_0| < 10^{-4}\mu_0$, comparing with their electric counter parts, largely because of the nonexistence of magnetic monopoles.

2.1.1 The Wave Equation

The coupled electric and magnetic fields in Maxwell's equations are disentangled by taking the curl of Eqs. 2.3 and 2.4 and using the linear relations of Eqs. 2.6 and 2.7:

$$\nabla \times (\nabla \times \mathbf{E}) + \epsilon\mu \frac{\partial^2 \mathbf{E}}{\partial t^2} = -\mu \frac{\partial \mathbf{J}_f}{\partial t}, \tag{2.8}$$

$$\nabla \times (\nabla \times \mathbf{H}) + \epsilon\mu \frac{\partial^2 \mathbf{H}}{\partial t^2} = \nabla \times \mathbf{J}_f. \tag{2.9}$$

These are the most general wave equations for $\mathbf{E}$ and $\mathbf{H}$. Using the vector identity

$$\nabla \times (\nabla \times \mathbf{A}) = \nabla(\nabla \mathbf{A}) - \nabla^2 \mathbf{A} \tag{2.10}$$

with Eqs. 2.1 and 2.2 we can rewrite the wave equations as

$$\nabla^2 \mathbf{E} - \epsilon\mu \frac{\partial^2 \mathbf{E}}{\partial t^2} = \mu \frac{\partial \mathbf{J}_f}{\partial t} + \frac{1}{\epsilon} \nabla \rho_f, \tag{2.11}$$

$$\nabla^2 \mathbf{H} - \epsilon\mu \frac{\partial^2 \mathbf{H}}{\partial t^2} = -\nabla \times \mathbf{J}_f. \tag{2.12}$$

Assuming $\mathbf{J}_f$ is linear with $\mathbf{E}$,

$$\mathbf{J}_f = \sigma \mathbf{E}, \tag{2.13}$$

where σ is the electric conductivity, and neglecting charge density fluctuations, i.e., $\nabla \rho_f = 0$, we simplify the wave equation for $\mathbf{E}$ as

$$\nabla^2 \mathbf{E} = \sigma\mu \frac{\partial \mathbf{E}}{\partial t} + \epsilon\mu \frac{\partial^2 \mathbf{E}}{\partial t^2}. \tag{2.14}$$

Here σ and ϵ are real and independent. The wave equation for $\mathbf{H}$ takes an identical form. These time-varying fields are closely intertwined by Maxwell's equations: if one is known, the other is fully determined. The coupled entity of the two fields is called an *electromagnetic wave*.

If the material is a dielectric or an insulator, the wave equation takes the universal form

$$\nabla^2 \mathbf{E} = \epsilon\mu \frac{\partial^2 \mathbf{E}}{\partial t^2} = \frac{1}{v^2} \frac{\partial^2 \mathbf{E}}{\partial t^2}, \tag{2.15}$$

which signifies that electromagnetic waves propagate in homogeneous media at a speed

$$v = \frac{1}{\sqrt{\epsilon\mu}} = \frac{c}{n}, \tag{2.16}$$

where $c \left(= 1/\sqrt{\epsilon_0 \mu_0}\right)$ is the speed of light in free space and $n \left(= \sqrt{\epsilon/\epsilon_0}\right)$ is the refractive index, assuming $\mu = \mu_0$.

General solutions of the wave equation are linearly-polarized monochromatic plane waves:

$$\mathbf{E}(\mathbf{r}, t) = \mathbf{E}_0 e^{i(\mathbf{k}\cdot\mathbf{r} - \omega t)} \quad \text{and} \quad \mathbf{H}(\mathbf{r}, t) = \mathbf{H}_0 e^{i(\mathbf{k}\cdot\mathbf{r} - \omega t)}, \tag{2.17}$$

where $\mathbf{k}$ is the wave vector and ω is the angular frequency. From Maxwell's equations we can draw the relations between $\mathbf{E}$ and $\mathbf{H}$ associated with $\mathbf{k}$ and ω. Substituting the plane waves into $\nabla \cdot \mathbf{E} = 0$ and $\nabla \cdot \mathbf{B} = 0$ we obtain

$$\mathbf{k} \cdot \mathbf{E} = 0 \quad \text{and} \quad \mathbf{k} \cdot \mathbf{H} = 0. \tag{2.18}$$

This means that $\mathbf{E}$ and $\mathbf{H}$ are both perpendicular to the wave vector, that is, electromagnetic waves are transverse. The curl equations give the relation

$$\mathbf{k} \times \mathbf{E} = \omega\mu \mathbf{H}. \tag{2.19}$$

Inserting Eq. 2.17 into Eq. 2.15 we obtain the dispersion relation

$$k^2 = \epsilon\mu\omega^2. \tag{2.20}$$

As ϵ and μ quantify the electromagnetic properties of the material, the dispersion relation governs how the wave propagates in the medium. For a non-magnetic medium, the wavenumber k is related to the wavelength λ by the relation

$$k = \frac{2\pi}{\lambda} = n\frac{\omega}{c}. \tag{2.21}$$

The energy flux of an electromagnetic wave is the time-averaged Poynting vector

$$\langle \mathbf{S} \rangle = \frac{1}{2} \mathbf{E} \times \mathbf{H}^* = \frac{1}{2} v\, \epsilon |E_0|^2 \mathbf{e}_k, \tag{2.22}$$

where $\mathbf{e}_k (= \mathbf{k}/k)$ is a unit vector in the direction of the wave propagation. The magnitude of the energy flux,

$$I = |\langle \mathbf{S} \rangle| = \frac{1}{2} v\, \epsilon |E_0|^2, \tag{2.23}$$

is the radiation intensity, which is the measurement quantity of typical light detectors. A commonly used unit of light intensity is $\mathrm{W/cm^2}$.

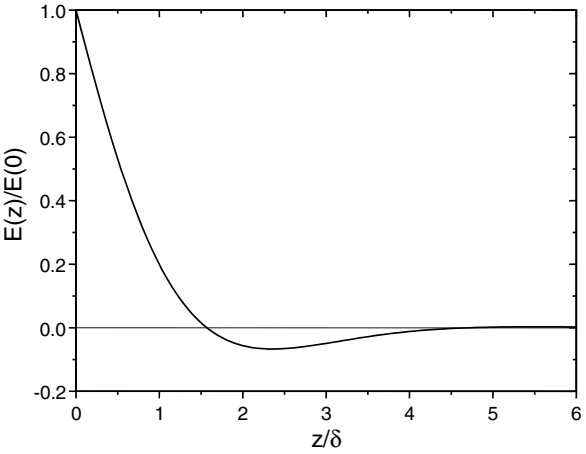

Fig. 2.1. Electric field decay in a conductor

In a conducting medium, general solutions of the wave equation, Eq. 2.14, also take the form of the plane waves in Eq. 2.17. Even Eqs. 2.18 and 2.19 are still valid. Wave propagation in a conductor is, however, quite different from that in a dielectric medium. If the medium has a very large conductivity such that $\sigma \ll \omega\epsilon$, the wave equation leads to the dispersion relation

$$k^2 \approx i\sigma\mu\omega. \tag{2.24}$$

Evidently the amplitude of the wave vector is a complex number,

$$k = k_R + ik_I \approx \sqrt{\frac{\omega\mu\sigma}{2}}(1+i). \tag{2.25}$$

This means that when an electromagnetic wave is incident on a conductor the field decays exponentially with an attenuation length δ, which is called the penetration depth or the skin depth:

$$\delta = \sqrt{\frac{2}{\omega\mu\sigma}} \ . \tag{2.26}$$

Typical metals behave like an ideal conductor for THz waves. For example, the skin depth of copper is $\delta \approx 0.07$ μm for the frequency $\nu(= \omega/2\pi) =$ 1 THz, which is almost negligible when compared to the free-space wavelength, 300 μm.

2.1.2 Reflection and Transmission

When an electromagnetic wave reflects from and transmits through an interface of two linear dielectric media, both **E** and **H** obey the boundary condition

that the parallel components of the vector fields are continuous across the interface. An apparent ramification of the boundary condition is Snell's law

$$n_1 \sin\theta_1 = n_2 \sin\theta_2, \tag{2.27}$$

where $n_{1,2}$ are the refractive indices of the media and $\theta_{1,2}$ are the angle of incidence and the angle of refraction.

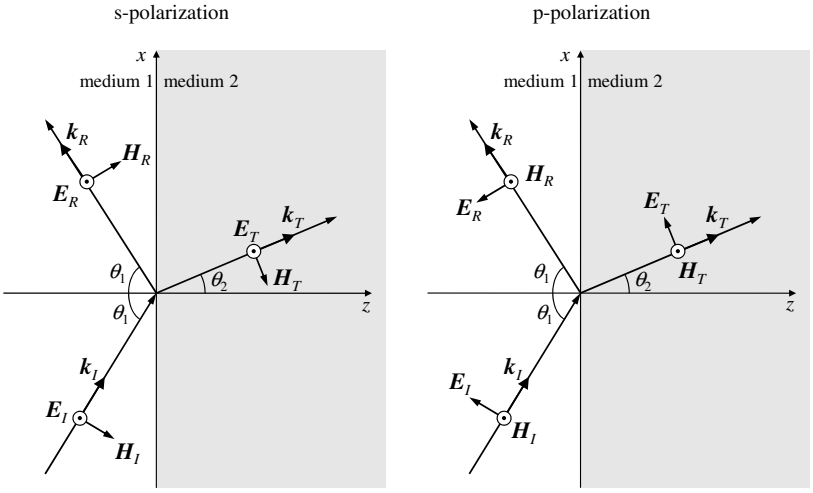

Fig. 2.2. Reflection and transmission of s- and p-polarized electromagnetic waves

Figure 2.2 illustrates the incident, reflected, and transmitted waves on a plane of incidence. S-polarization denotes the case when the polarization of the incident wave is perpendicular to the plane of incidence, and p-polarization is when the polarization of the incident wave is parallel to the plane of incidence. Eventually, the boundary conditions determine the ratios of the reflected and transmitted field amplitudes to the incident field amplitude. These relations are expressed in the Fresnel equations:

$$\frac{E_{R,s}}{E_{I,s}} = \frac{n_1\cos\theta_1 - n_2\cos\theta_2}{n_1\cos\theta_1 + n_2\cos\theta_2} \quad \text{and} \quad \frac{E_{T,s}}{E_{I,s}} = \frac{2n_1\cos\theta_1}{n_1\cos\theta_1 + n_2\cos\theta_2} \tag{2.28}$$

for s-polarization and

$$\frac{E_{R,p}}{E_{I,p}} = \frac{n_2\cos\theta_1 - n_1\cos\theta_2}{n_2\cos\theta_1 + n_1\cos\theta_2} \quad \text{and} \quad \frac{E_{T,p}}{E_{I,p}} = \frac{2n_1\cos\theta_1}{n_2\cos\theta_1 + n_1\cos\theta_2} \tag{2.29}$$

for p-polarization.

Reflectivity R is defined as the fraction of incident radiation power that reflects from the boundary, and transmittance T that transmits through. Since

the radiation intensity striking the interface is the normal component of the Poynting vector $\langle \mathbf{S} \rangle \cdot \mathbf{e}_k$, the reflectivity and the transmittance are given as

$$R = \frac{|E_R|^2}{|E_I|^2} \quad \text{and} \quad T = \frac{n_2 |E_T|^2}{n_1 |E_I|^2}. \tag{2.30}$$

Figure 2.3 shows an example of the reflectivity of s- and p-polarized waves versus the angle of incidence for n_1=1 and n_2=2. The reflectivity of p-polarization is completely expunged at *Brewster's angle*,

$$\theta_B = \tan^{-1}\left(\frac{n_2}{n_1}\right). \tag{2.31}$$

If medium 1 is optically denser than medium 2, i.e., $n_1 > n_2$, reflectivity becomes unity for

$$\theta_1 > \sin^{-1}\left(\frac{n_2}{n_1}\right). \tag{2.32}$$

This phenomenon is called *total internal reflection*.

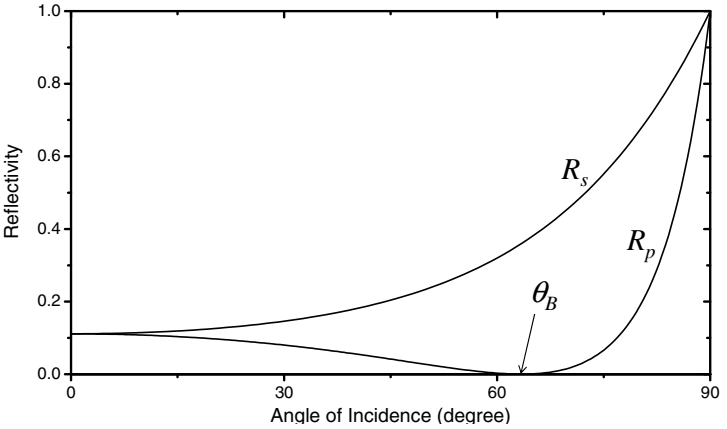

Fig. 2.3. Reflectivity of s- and p-polarization versus angle of incidence

The same boundary conditions are applied to a conducting surface. Consider an electromagnetic wave incident on an interface of air and a conductor with normal angle. Eq. 2.28 is still valid if we substitute n_2 with a complex index of refraction,

$$\tilde{n} = \frac{ck}{\omega} = c\sqrt{\frac{\mu\sigma}{2\omega}}(1+i), \tag{2.33}$$

using Eq. 2.25. Due to the large conductivity, $|\tilde{n}| \gg 1$,

$$E_R = \frac{1-\tilde{n}}{1+\tilde{n}} E_I \cong -E_I, \tag{2.34}$$

$$E_T = \frac{2}{1+\tilde{n}} E_I \cong 0. \tag{2.35}$$

The reflectivity is close to unity, and very little energy is dissipated into the conducting medium.

2.1.3 Coherent Transmission Spectroscopy

Coherent THz spectroscopy in a transmission geometry is a commonly used technique to measure the optical constants of materials. The coherent detection scheme measuring both the amplitude and phase of THz fields warrants simultaneous determination of the real and imaginary part of a dielectric function $\epsilon_r(\omega)$ or a conductivity $\sigma(\omega)$.

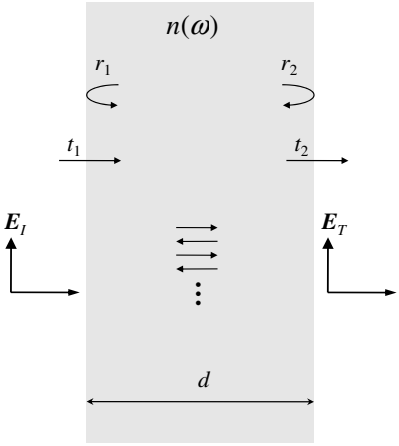

Fig. 2.4. Transmission of an electromagnetic wave through a flat single-layer of material with a complex index of refraction $\tilde{n}(\omega)$ and a thickness d. r_1 and r_2 are the reflection coefficients at the entrance and exit surfaces, respectively, and t_1 and t_2 are the transmission coefficients.

Figure 2.4 illustrates a normal-incident electromagnetic wave passing through a single-layer of material with a thickness d and a complex index of refraction

$$\tilde{n}(\omega) = n(\omega) + i\kappa(\omega). \tag{2.36}$$

Inside the layer some parts of the wave undergo multiple reflections at the interfaces before they transmit through. Ultimately the total transmission is the superposition of all the parts having endured multiple reflections. Thus, the transmitted field E_T can be expressed as

$$\begin{aligned} E_T &= E_I t_1 t_2 e^{i\phi_d} + E_I t_1 t_2 e^{i\phi_d} \cdot \left(r_1 r_2 e^{2i\phi_d}\right) + \cdots \\ &= E_I t_1 t_2 e^{i\phi_d} \sum_{m=0}^{\infty} \left(r_1 r_2 e^{2i\phi_d}\right)^m \\ &= \frac{E_I t_1 t_2 e^{i\phi_d}}{1 - r_1 r_2 e^{2i\phi_d}}, \end{aligned} \tag{2.37}$$

where

$$r_1(\omega) = r_2(\omega) = \frac{\tilde{n}(\omega) - 1}{\tilde{n}(\omega) + 1}, \tag{2.38}$$

$$t_1(\omega) = \frac{2}{\tilde{n}(\omega) + 1}, \tag{2.39}$$

$$t_2(\omega) = \frac{2\tilde{n}(\omega)}{\tilde{n}(\omega) + 1}, \tag{2.40}$$

obtained from Eq. 2.28 with the incident angle $\theta_1 = 0$, are the reflection and transmission coefficients at the entrance and exit surfaces, and

$$\phi_d(\omega) = \tilde{n}(\omega)\frac{\omega}{c}d \tag{2.41}$$

is the phase shift while the wave propagates a distance d within the material. What we actually measure is the complex transmission coefficient $t(\omega)$ with the amplitude $|t(\omega)|$ and the phase $\Phi(\omega)$, which is expressed as

$$\begin{aligned} t(\omega) &= |t(\omega)| e^{\Phi(\omega)} \\ &= \frac{E_T(\omega)}{E_I(\omega)} = \frac{4\tilde{n}(\omega) e^{i\phi_d(\omega)}}{\left[\tilde{n}(\omega) + 1\right]^2 - \left[\tilde{n}(\omega) - 1\right]^2 e^{2i\phi_d(\omega)}} \end{aligned} \tag{2.42}$$

in terms of $\tilde{n}(\omega)$. $\tilde{n}(\omega)$ is determined by fitting the transmission data to Eq. 2.42.

The complex dielectric function

$$\epsilon_r(\omega) = \left[\tilde{n}(\omega)\right]^2 = \epsilon_{r1}(\omega) + i\epsilon_{r2}(\omega) \tag{2.43}$$

and the complexity conductivity

$$\sigma(\omega) = \sigma_1(\omega) + i\sigma_2(\omega) \tag{2.44}$$

have the relation

$$\sigma_1(\omega) = -\epsilon_0 \omega\, \epsilon_{r2}(\omega), \tag{2.45}$$

$$\sigma_2(\omega) = \epsilon_0 \omega \left[\epsilon_{r1}(\omega) - \epsilon_{r1}(\infty)\right], \tag{2.46}$$

where $\epsilon_{r1}(\infty)$ is the dielectric constant in the high-frequency limit.

2.1.4 Absorption and Dispersion

Frequency dispersion refers to the phenomenon in which waves of different frequencies propagate at different speeds. Dispersion, together with absorption, characterizes how media respond to external electromagnetic fields. All electromagnetic phenomena involve the interaction of fields with charged particles, electrons and nuclei at a microscopic scale, in matter. Electromagnetic waves force charged particles to move; their accelerated motion induces radiation. The effects of magnetic fields on naturally occurring materials are mostly negligible and the amplitude of the electron motions are usually very small. Consequently, electromagnetic properties of a medium are dominated by electric dipoles induced by the applied electric fields. In the linear optical regime, the electric dipole moments are proportional to the amplitude of the applied electric fields.

The classical Lorentzian model provides a good qualitative description of this phenomenon. Assuming that a bound charge oscillates about its equilibrium position with a very small amplitude, we model the system as a simple harmonic oscillator. Figure 2.5 illustrates the Lorentzian harmonic oscillator model. The potential energy of the charged particle is quadratic for small displacements from equilibrium. The size of the oscillator is much smaller than the wavelength of the applied field, hence the electric field is constant near the equilibrium position for a given time t.

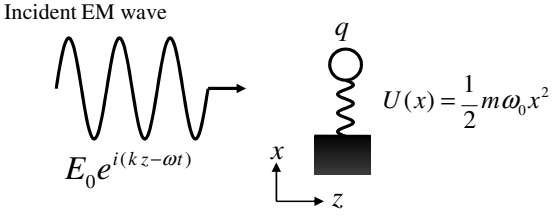

Fig. 2.5. The classical Lorentzian model accounts for the optical response of bound electrons in dielectric media.

When the monochromatic wave

$$E(t) = E_0 e^{-i\omega t} \tag{2.47}$$

of angular frequency ω, polarized along the x axis, interacts with the charge q, its equation of motion is expressed as

$$\frac{d^2x}{dt^2} + \gamma \frac{dx}{dt} + \omega_0^2 x = \frac{q}{m} E(t), \tag{2.48}$$

where q and m are the charge and the mass. γ and ω_0 are the damping constant and the resonant frequency, respectively. The solution of the equation of motion is

$$x(t) = x_0 e^{-i\omega t}, \quad \text{where} \quad x_0 = \frac{q}{m} \frac{E_0}{\omega_0^2 - \omega^2 - i\omega\gamma}. \tag{2.49}$$

The electric dipole moment of the harmonic oscillator is

$$p(t) = qx(t). \tag{2.50}$$

We suppose that a medium has N oscillators per unit volume, then the electric polarization is given by

$$P(t) = Nqx(t) = \frac{Nq^2}{m} \frac{E_0 e^{-i\omega t}}{\omega_0^2 - \omega^2 - i\omega\gamma} \equiv \epsilon_0 \chi_e(\omega) E_0 e^{-i\omega t}, \tag{2.51}$$

where $\chi_e(\omega)$ denotes the linear electric susceptibility of the medium. Inserting Eq. 2.51 into Eq. 2.6 we obtain the dielectric constant of the medium

$$\epsilon_r(\omega) \equiv \frac{\epsilon(\omega)}{\epsilon_0} = 1 + \chi_e(\omega) = 1 + \frac{Nq^2}{m\epsilon_0} \frac{1}{\omega_0^2 - \omega^2 - i\omega\gamma}\ . \tag{2.52}$$

The real and imaginary parts of the complex dielectric constant are written as

$$\Re\left[\epsilon_r\right] - 1 = \frac{Nq^2}{m\epsilon_0} \frac{\omega_0^2 - \omega^2}{\left(\omega_0^2 - \omega^2\right)^2 + \omega^2\gamma^2}, \tag{2.53}$$

$$\Im\left[\epsilon_r\right] = \frac{Nq^2}{m\epsilon_0} \frac{\omega\gamma}{\left(\omega_0^2 - \omega^2\right)^2 + \omega^2\gamma^2}. \tag{2.54}$$

Figure 2.6 shows characteristic dielectric dispersion in the vicinity of the resonant frequency. This medium is dispersive because its response to an external electromagnetic wave depends on frequency. The imaginary part of the dielectric constant indicates that absorption is maximized at the resonant frequency, and the bandwidth is $\sim \gamma$.

From the dispersion relation of Eq. 2.20 we get the complex amplitude of the wave vector

$$k(\omega) = k_R(\omega) + ik_I(\omega) = \sqrt{\epsilon_r(\omega)}\frac{\omega}{c}, \tag{2.55}$$

which governs how the wave propagates in the medium. The plane wave propagating along the z-axis is written as

$$\mathbf{E}(z,t) = \mathbf{E}_0 e^{i(kz-\omega t)} = \mathbf{E}_0 e^{-\frac{\alpha}{2}z} e^{-i\omega\left(t-\frac{n}{c}z\right)}. \tag{2.56}$$

The radiation intensity exponentially decays with an absorption coefficient

$$\alpha(\omega) = 2\Im[k(\omega)], \tag{2.57}$$

and the wave propagates with the phase velocity

$$v = \frac{n(\omega)}{c} = \frac{\Re[k(\omega)]}{\omega}. \tag{2.58}$$

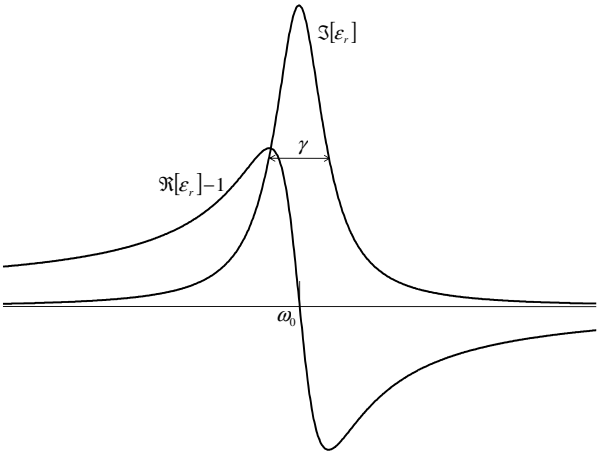

Fig. 2.6. Dielectric dispersion at a resonance.

2.1.5 Plasma Frequency

Consider the interaction of electromagnetic waves with a system in which charges move freely, and scattering between the particles is negligible. Doped semiconductors or plasmas may behave in such a way upon incidence of THz radiation. Substituting $\omega_0 = 0$ and $\gamma = 0$ into Eq. 2.52 we get the dielectric constant,

$$\epsilon_r(\omega) = 1 - \frac{\omega_p^2}{\omega^2}, \tag{2.59}$$

where

$$\omega_p = \sqrt{\frac{Nq^2}{m\epsilon_0}} \tag{2.60}$$

is the *plasma frequency*. The dispersion relation,

$$ck = \sqrt{\omega^2 - \omega_p^2}, \tag{2.61}$$

indicates that waves can propagate through the medium for $\omega > \omega_p$, while it decays with the absorption coefficient,

$$\alpha(\omega) = \frac{2}{c}\sqrt{\omega_p^2 - \omega^2}, \tag{2.62}$$

for $\omega < \omega_p$. A typical electron density, 10^{16} cm^{-3}, of laboratory plasmas and doped semiconductors corresponds to $\omega_p \cong 6$ THz.

2.1.6 Electric Dipole Radiation

Electromagnetic waves are generated by accelerating charges and time-varying currents. In the present section, we discuss the emission of radiating fields from